Journal of Nuclear Materials 377 (2008) 136–140

Contents lists available at ScienceDirect

Journal of Nuclear Materials

journal homepage: www.elsevier.com/locate/jnucmat

Modeling and simulation of irradiation hardening in structural ferritic steels for advanced nuclear reactors

Chaitanya Deo [a,*], Carlos Tomé [b], Ricardo Lebensohn [b], Stuart Maloy [b]

[a] Nuclear and Radiological Engineering Program, George W. Woodruff School of Mechanical Engineering, Georgia Institute of Technology, Atlanta, GA 30332, United States
[b] Los Alamos National Laboratory, MS-H809, Los Alamos, NM 87545, United States

ARTICLE INFO

PACS:
62.20.−x
62.20.Fe
61.80.Hg
61.80.Az

ABSTRACT

Hardening and embrittlement are controlled by interactions between dislocations and irradiation induced defect clusters. In this work we employ the visco plastic self consistent (VPSC) polycrystalline code in order to model the yield stress dependence in ferritic steels on the irradiation dose. We implement the dispersed barrier hardening model in the VPSC code by introducing a hardening law, function of the strain, to describe the threshold resolved shear stress required to activate dislocations. The size and number density of the defect clusters varies with the irradiation dose in the model. We find that VPSC calculations show excellent agreement with the experimental data set. Such modeling efforts can both reproduce experimental data and also guide future experiments of irradiation hardening.

Published by Elsevier B.V.

1. Introduction

Radiation hardening and embrittlement that occurs in metals irradiated at low temperatures (below ~0.3 T_m, where T_m is the melting temperature) is an important technical challenge for advanced nuclear energy systems [1]. Hardening and embrittlement are controlled by interactions between dislocations and irradiation induced defect clusters. For some materials applications, radiation damage and relatively large amounts of helium generated during the irradiation damage process are major issues affecting materials durability and performance.

The effect of irradiation on mechanical properties of structural materials is illustrated in Fig. 1, which shows the stress–strain curves of unirradiated and irradiated T91 (9Cr 1Mo) ferritic steel. The specimens were tensile tested following irradiation for six months (maximum dose is ~8 dpa) at 50–80 °C in a spallation proton and neutron flux at the end of the 800 MeV/1 mA LANSCE accelerator. Details of the testing procedures employed can be found in [2]. Fig. 2 plots the yield stress dependence to irradiation dose for these specimens. The results show that the yield stress sharply increased with increasing irradiation dose and the uniform elongation dropped precipitously to less than 1% after slightly more than 0.1 dpa of irradiation dose. Such hardening features are detrimental to the performance of the steel as structural materials in advanced nuclear energy systems.

In this work we employ the visco plastic self consistent (VPSC) polycrystalline code [3] in order to model the yield stress dependence in ferritic steels on the irradiation dose. VPSC is a computer code which simulates the plastic deformation of polycrystalline aggregates subjected to external strains and stresses. VPSC accounts for full anisotropy in properties and response of the single crystals and the aggregate. VPSC is based on the physical deformation mechanisms of slip and twinning, and accounts for grain interaction effects. In addition to providing the macroscopic stress–strain response, it accounts for the evolution of hardening and texture associated with plastic forming of metals, although for the present application we are not concerned with evolution, but only with the initial yield stress as a function of radiation dose.

2. Dispersed barrier hardening

In order to describe the nature of the yield stress dependence on the irradiation dose, we implemented a new microstructural model at the grain level in the VPSC code. The model assumes that hardening is affected by the presence of the defects and defect clusters produced by irradiation. These defects interact with the pre-existing dislocations in the microstructure leading to an increase in the critical stress necessary to move the dislocations. This leads to an increase in the overall yield stress of the material.

Defects are treated as barriers to the motion of dislocations. Two approximate dislocation barrier models have historically been used to describe radiation hardening in metals [1] and are reviewed in [4,5]. The dispersed barrier model [6] is based on straightforward geometrical considerations for obstacles intersecting the dislocation glide plane and it is most appropriate for strong obstacles. An alternative hardening relationship was developed by Friedel–Kroupa–Hirsch (FKH) for weak obstacles [7,8], where the

* Corresponding author.
E-mail address: chaitanya.deo@me.gatech.edu (C. Deo).

0022-3115/$ - see front matter Published by Elsevier B.V.
doi:10.1016/j.jnucmat.2008.02.064

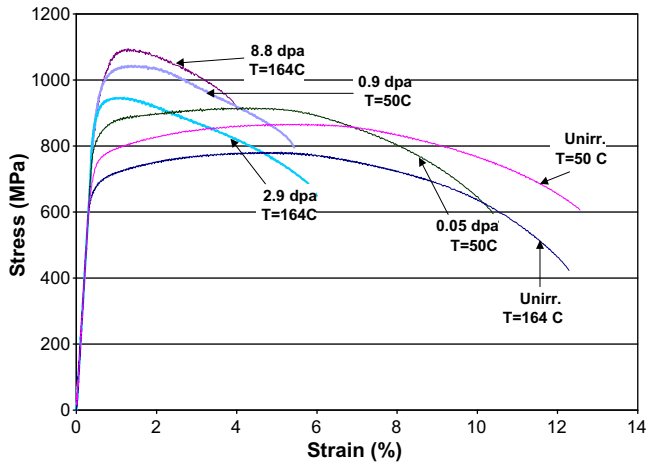

Fig. 1. Stress–strain curves for unirradiated and irradiated ferritic steels (T91) [2].

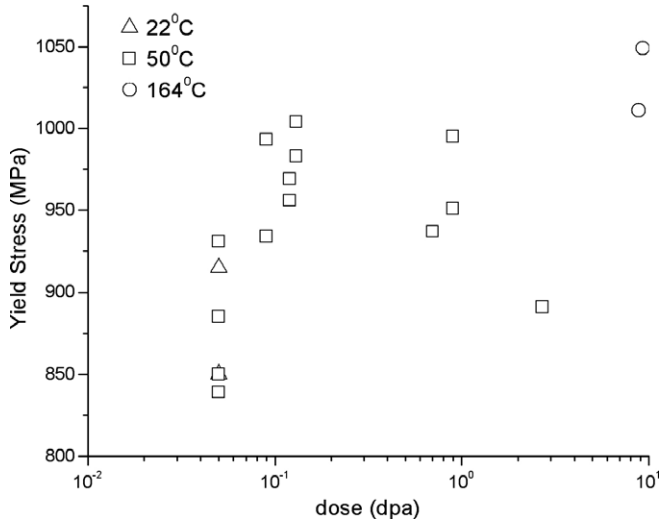

Fig. 2. Yield stress variation with dose for the irradiated and unirradiated ferritic steel specimen [2]. Unirradiated values are not shown. Irradiations were performed at three different temperatures 22 °C (open triangles), 50 °C (open squares) and 164 °C (open circles).

effective interparticle spacing is increased compared to the planar geometric spacing due to less extensive dislocation bowing prior to obstacle breakaway. Using the simple approximation for dislocation line tension, the functional dependence of polycrystalline yield strength increase on defect cluster size and density for these two limiting cases is given by the following equations:

$$\Delta\sigma = M\alpha\mu b\sqrt{Nd}, \tag{1}$$

$$\Delta\sigma = \frac{1}{8}M\mu bN^{\frac{2}{3}}d, \tag{2}$$

Eq. (1) corresponds to the dispersed barrier hardening model and Eq. (2) to the FKH model. In the two equations, $\Delta\sigma$ is the change in the yield stress, M is the Taylor factor (3.06 for non-textured BCC and FCC metals), α is the defect cluster barrier strength, μ is the shear modulus, b is the Burgers vector of the primary glide dislocations, and N and d are the defect cluster density and diameter.

Most radiation hardening studies have used the dispersed barrier model (Eq. (1)) for data interpretation, and in this work we find that it provides a better representation of our experimental results. However, the FKH model (Eq. (2)) may be more appropriate for many radiation-induced small defect clusters which are weak obstacles to dislocation motion. According to some early analyses [4], the FKH model is adequate for barrier strengths up to 1/4 of the Orowan (impenetrable obstacle) limit, i.e., $\alpha < 0{:}25$, and the dispersed barrier model is more appropriate for barrier strengths of $0.25 < \alpha < 1$. Typical experimental values of the defect cluster barrier strength for copper and austenitic stainless steel neutron-irradiated and tested near room temperature are $\alpha = 0.15$–0.2 [9]. The reported barrier strengths for the visible defect clusters in BCC metals [10] are $\alpha = 0.4$ or higher. It is possible that hardening from nanovoids in the BCC metals might cause one to overestimate the reported barrier strength for the visible defect clusters.

We implemented the dispersed barrier hardening model in the VPSC code. It is possible to introduce a hardening law that is a function of the strain to describe the threshold resolved shear stress required to activate dislocations. In the present application, however, evolution is not simulated and only the initial threshold is required. We assume that the initial critical resolved shear stress (CRSS) in each grain is affected by irradiation according to the dispersed barrier hardening law and follows the Orowan expression,

$$\tau = \tau_0 + \alpha\mu b\sqrt{Nd}, \tag{3}$$

where τ is the initial CRSS, τ_0 is the unirradiated initial CRSS and the other parameters have the same meaning as in Eqs. (1) and (2). Observe that the Taylor factor is not included in Eq. (3), since the geometric crystal orientation effects are accounted for by the polycrystal model. The critical stress τ is assigned to the 12 (1 1 0)[1 1 1] and the 12 (1 1 0)[1 1 2] slip systems of the BCC structure. The initial texture of the rolled ferritic steel is represented using 1000 crystallographic orientations. Each orientation is treated as an ellipsoidal inclusion embedded in and interacting with the effective medium that represents the aggregate. An incremental strain is enforced along the rolling direction, while leaving the lateral strains unconstrained. The stress and the strain is different from grain to grain, and the macroscopic (yield) stress is given by the average over all orientations.

Through Eq. (3) the model will include a dependence of the yield stress on the damage created due to radiation. Radiation damage is usually expressed as a statistical quantity describing the average number of displacements for each atom (dpa). The dpa influences the yield stress by determining the number density and the size of the defect clusters (obstacles) that impede the path of the dislocations and increase the critical stress required to move the dislocation.

3. Defect clusters

It has commonly been assumed that the defect cluster density in irradiated metals increases linearly with increasing dose, up to the onset of cascade overlap which causes a saturation in the cluster density [5,11,12]. However, in several pure FCC metals the defect accumulation as measured by electrical resistivity [9,12] or transmission electron microscopy [9,13] often appears to exhibit an intermediate dose regime where the defect cluster density is proportional to the square root of dose. The defect accumulation behavior was found to be linear at very low doses (<0.0001 dpa, where the probability of uncorrelated point defect recombination is negligible), and proportional to the square root of dose at higher doses. According to simple kinetic models such as the unsaturable trap model [14,15], the critical dose for transition from linear to square root behavior depends on specimen purity. In this model, the transition to square root accumulation behavior can be delayed up to high doses if impurity trapping of migrating interstitial-type defects is dominant compared to interstitial–interstitial or interstitial–vacancy reactions.

The dependence on irradiation dose (expressed as dpa) of the defect cluster density (N) and the defect diameter (d) are taken from atomic level kinetic Monte Carlo (kMC) simulations and experimental observations [16–18] The kMC model takes atomic level information of the migration energies and jump attempt frequencies of irradiation induced defects (interstitials, vacancies) and transmutation products (e.g., helium under high energy proton irradiation), and evolves the microstructure according to the rates of migration of these defects. The defects are allowed to cluster, and new irradiation damage is introduced during the simulation according to the irradiation dose rate. Our kMC simulations predict that the number density varies as the square root of the displacements per atom for the case of bcc iron irradiated up to 1 dpa by high energy proton irradiation.

The size dependence on irradiation dose is more complicated as the kMC simulations provide an entire distribution of defect cluster sizes. A single value of d as a function of dose is still a simplification of the kMC results. The defect size usually increases with increasing dose (dpa) and can be fit by a power law; however the exponent of the power law expression can vary from 0 to 0.5 depending on initial simulation conditions (dose rate, temperature) and the defect cluster size considered. At low dpa, the exponent of the power law dependence is small for all defect sizes and increases at higher dpa.

Here we consider the density of defects N to vary as the square root of the dpa while two cases of size dependence are considered, one in which the size is invariant with the dose (dpa) while the other in which the defect size varies as the square root of the dose. Additional systematic work is needed to confirm the presence and to understand the physical mechanisms responsible for this square root fluence-dependent defect cluster accumulation regime.

4. Results

We employ the VPSC polycrystalline code to model the yield stress dependence on the irradiation dose in ferritic steels. Two sets of experimental data are used for comparison, one due to Maloy and co-workers [2] and the other due to Dai and co-workers [19]. The first data set was generated by irradiations performed at the Los Alamos Neutron Science Center (LANSCE) on ferritic T91 (9Cr 1Mo) steels followed by tensile tests on the irradiated specimens. Damage introduced is of the order of 1 dpa. The other set of data [20,21] was generated by 800 MeV proton irradiation of T91 steel samples at the Paul Scherrer Institute. Irradiation dose in that case was much higher (up to 10 dpa).

The initial texture of the rolled ferritic T91 polycrystal was measured using X-rays. Fig. 3 shows a pole figure corresponding to 1000 weighted grains used to represent the texture. The texture is relatively weak and, since the tensile tests were conducted in the rolling direction (RD), the VPSC simulations were also carried out along such direction. We also simulate the results that would be obtained if the test were done along the transverse direction (TD). The difference between both cases will evidence the anisotropy in the mechanical response of irradiated material associated with texture. Due to the weak texture of this particular sample, the tensile responses along RD and TD are very similar. Material parameters for the hardening law are taken to correspond to ferritic steels, namely, the dislocation-defect interaction strength $\alpha = 0.5$, the shear modulus $\mu = 82$ GPa and the burgers vector is that of the $1/2\ \langle 1\,1\,1\rangle$ screw dislocation ($b \sim 0.25$ nm).

Figs. 4(a) and 4(b) show the yield stress dependence for the case of the T91 ferritic steels irradiated at low dpa (up to 1 dpa). The initial critical resolved shear stress in the VPSC code is adjusted so that the unirradiated yield stress of the material is reproduced. In Fig. 4(a), the defect cluster size is kept constant at a value of 4 nm, while the number density is varied as the square root of the dpa

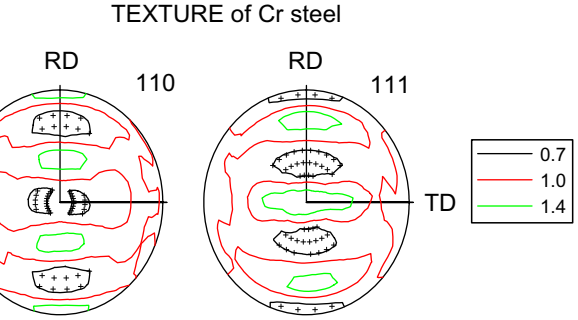

Fig. 3. Pole figures corresponding to the input texture used in the VPSC calculations. RD and TD are the rolling and the transverse directions, respectively.

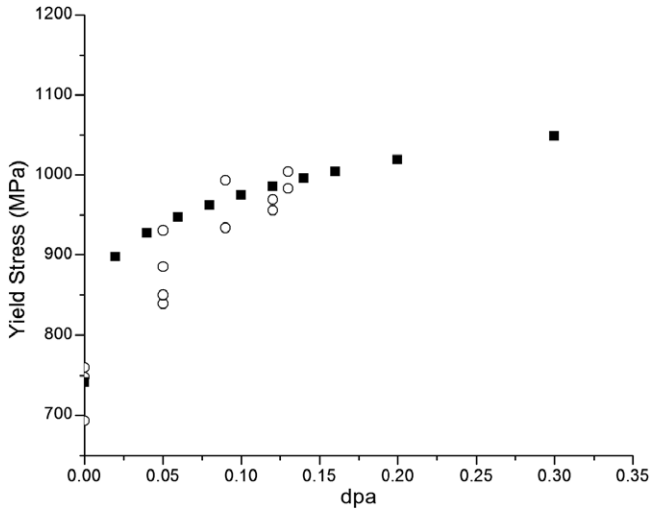

Fig. 4(a). Variation of the yield stress with dpa for the case of T91 steel subject to low radiation. The defect cluster density varies with the square root of the irradiation dose (dpa) while the defect cluster size is not sensitive to irradiation dose. Filled squares are the VPSC calculations, open circles are the experimental data [2].

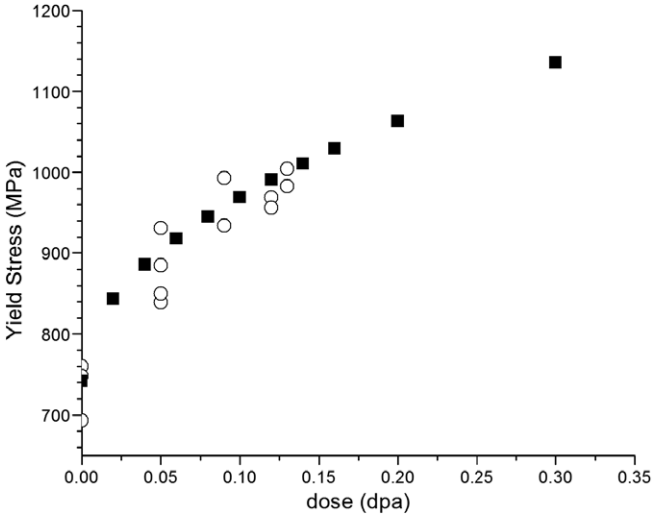

Fig. 4(b). Variation of the yield stress with dpa for the case of T91 steel subject to low radiation. The defect cluster size varies as the square root of the irradiation dose (dpa). Filled squares are the VPSC calculations, open circles are the experimental data [2].

$$N = A\ \mathrm{nm}^{-3}\ \mathrm{dpa}^{\frac{1}{2}} \quad (4)$$

The value of the constant A is assumed to be 1×10^{-3} nm^{-3} which is consistent with atomistic kinetic Monte Carlo calculations. In Fig. 4(b), the initial defect size is varied as the square root of the dpa,

$$d = B\ \mathrm{nm}\ \mathrm{dpa}^{-\frac{1}{2}} \quad (5)$$

The value of B is assumed to be 8 nm. These values are presently much higher than those from atomistic kinetic Monte Carlo calculations but the square root dependence of the number density and defect size is observed in the atomistic kinetic Monte Carlo calculations [17,22].

Both methods reproduce the increase in yield stress as a function of the dpa. In Fig. 4(a) there is large discrepancy in the low dpa (up to 0.1 dpa) dependence of the yield stress. In general, we find that VPSC calculations shown in Fig. 4(b) show excellent agreement with the experimental data set [2].

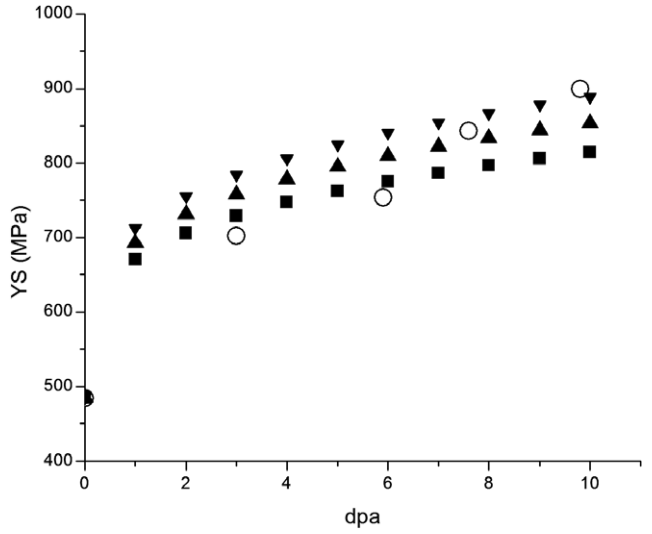

Fig. 5(a). Variation of the yield stress with dpa for the case of T91 steel subject to high levels of radiation. The defect cluster size is not sensitive to irradiation dose. Filled symbols are the VPSC calculations assuming defect cluster sizes of 4 nm (squares), 6 nm (up triangles) and 8 nm (down triangles); open circles are the experimental data [19].

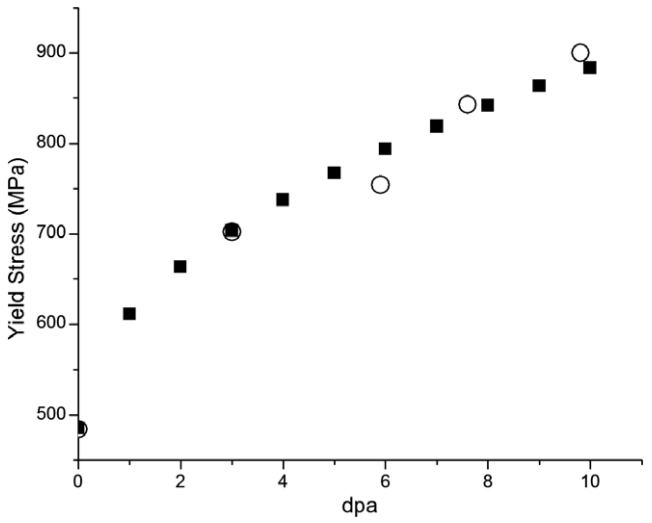

Fig. 5(b). Variation of the yield stress with dpa for the case of T91 steel subject to high levels of radiation. The defect cluster size is varied as the square root of the dpa. Filled squares are the VPSC calculations; open circles are the experimental data [19].

Figs. 5(a) and 5(b) show the yield stress dependence at high dpa for the case of the T91 ferritic steels irradiated at high dpa (up to 10 dpa). In Fig. 5(a), the VPSC calculations are performed with the defect cluster size held constant. Three values of d are used 4, 5 and 6 dpa. The number density is varied as the square root of the dpa as described in Eq. (4) with $A = 5 \times 10^{-5}$ nm^{-3}. We find that the overall increase in the yield stress as calculated by the VPSC code does not agree very well with the experimental data if the defect size is held constant (Fig. 5(a)).

In Fig. 5(b), the initial defect density is assumed to vary according to Eq. (4) and the initial defect size is varied as the square root of the dpa (Eq. (5)). The value of the constants A is 5×10^{-5} nm^{-3} and the value of B is taken from atomistic calculations and experimental observations to be 3.7 nm. We find that VPSC calculations shown in Fig. 5(b) are in very good agreement with the experimental data of Dai et al. [19].

5. Discussion and summary

The two cases considered ascribe different dependence of the change in stress with the dose. In the first case (Figs. 4(a) and 5(a)), it follows from Eqs. (3) and (4) that $\Delta\tau$ varies as the ¼ power of the dpa. In the second case (Figs. 4(b) and 5(b)), it follows from Eqs. (1), (4), and (5) that $\Delta\tau$ varies as the 1/2 power of the dpa. A square root dose dependence of radiation hardening would also arise from the dispersed barrier hardening model if the defect cluster density increased in direct proportion to dose and the defect size was independent of dose [1]. Such a model (linear number density dependence and no cluster size dependence) is often empirically used to describe the number density and size dependence on dpa. As mentioned before, experimental observations do not agree on the dose dependence of the number density or size. In some studies, the defect accumulation behavior was found to be linear at very low doses and proportional to the square root of dose at higher doses [9,11,21]. The existence of submicroscopic bubbles and defect clusters makes experimental evaluation of the dose dependence of the number density and size of defect clusters quite difficult.

Helium bubble size and density dependence may have implications for the consideration of irradiation hardening [23]. As the damage levels in structural materials increase, these materials show an increase in the yield stress. The increase in the yield stress is related to the interaction of dislocations with obstacles produced by the radiation damage and is expressed by Eqs. (1) and (2). The quantities N and d in these equations are the number density and diameter of the obstacles. If bubbles are assumed to interact with dislocation by such a relationship, the number density and the bubble size can be calculated by kMC calculations as shown in this paper and employed as parameters in continuum level plasticity calculations of irradiation hardening. However the nature of the interaction of the bubbles with dislocations is not known with as much certainty as the nature of the interactions of dislocations with interstitial defect clusters. Experimental observations suggest that the presence of helium does not affect the yield stress of the materials [2,24].

Helium bubbles do affect the embrittlement properties of the structural materials along the ductile brittle transition temperature (DBTT) [19,23–27]. In this study we have focused on the yield stress variation of the structural materials with irradiation dose. Other mechanical properties (ductility, DBTT, embrittlement) are also critically affected by the irradiation environment [26,27]. Most of these properties are related to features at the nanoscale: the

formation of bubbles and voids at grain boundaries or the increase in activation barriers for dislocations at due to changes in dislocation core structure at low temperature. Mechanical property changes are the macroscopic manifestations of these nanoscale phenomena. An effective modeling and simulation study of these phenomena should be capable of linking various length and time scales in order to reproduce these effects.

The link between the atomic level simulations and the VPSC calculations was established using the dispersed barrier hardening model. In this model, the vacancy/interstitial clusters produced in radiation cascades are assumed to act as barriers to the gliding dislocation in the slip plane and are therefore taken to be the main source of radiation hardening. A different model of radiation hardening postulates the formation of defect clouds along the length of the grown-in dislocation (see [4,5] for review). These clouds prevent the dislocation from acting as Frank Read dislocation sources and emitting more dislocations. Singh Ghoniem and Trinkaus [29,30] proposed the cascade induced source hardening model (CISH) ten years ago. The CISH model accounted for interstitial cluster formation during radiation cascade formation. Such cluster formation has been observed in molecular dynamics simulations. In the CISH model, glissile loops produced directly in cascades are assumed to decorate grown-in dislocations so they cannot act as dislocation sources. The yield stress is related to the breakaway stress which is necessary to pull the dislocation away from the clusters/loops decorating it. Various aspects of the model (main assumptions and predictions) have been investigated by these researchers using analytical calculations, 3-D dislocation dynamics and molecular dynamics simulations It will be our intention to investigate such recent radiation hardening mechanisms by including them to develop the links between the atomic level understanding of defect sizes and concentrations and the VPSC model of polycrystalline hardening. Such mechanisms may also be investigated by atomic level simulations of single dislocation motion in the presence of defect impurities.

Our VPSC calculations have maintained a constant value for the dislocation-defect interaction strength (α in Eq. (3)) independent of the defect size (d) and number density (N). Further work needs to be done in order to understand the relations between these quantities for the case of bcc iron and ferritic steels. Arsenlis and co-workers [28] have developed a dislocation density-based constitutive model for the mechanical behavior of irradiated Cu. Their plasticity model includes mechanisms for dislocation density growth and multiplication and for irradiation defect density evolution with dislocation interaction. The general behavior of the constitutive (homogeneous material point) model shows that as the defect density increases, the initial yield point increases and the initial strain hardening decreases. The final coarse-grained model is implemented into a finite element framework and used to simulate the behavior of tensile specimens with varying levels of irradiation induced material damage. The model has been applied to the case of irradiation damage in fcc Cu, where the predominant obstacles to dislocations are stacking fault tetrahedra. In the case of bcc metals and alloys, defect clusters, voids and loops are the predominant obstacles to dislocation motion.

In a manner similar to the approach of Arsenelis and co-workers [28], the VPSC model can be used to combine microstructural input from both experimental observations and model predictions to evaluate the contributions from multiple defect cluster types. Although not all of the relevant parameters are currently known, but such parameter-studies that can inform future atomic-scale studies of dislocation–obstacle interactions. The VPSC model could also incorporate experimentally observed defect cluster distributions, number densities to assess the effect of multiple defect types and distributions. A detailed multiscale study, wherein the dislocation-obstacle strength and the number density and size of defects are correlated to the increasing strain and each other, would then further explain the effect of irradiation on mechanical properties of ferritic steels.

The VPSC calculations provide a means to link atomistic first principles calculations to macroscopic observables. The formulation of the irradiation hardening law allows for the introduction of parameters such as the defect size and number density that can be calculated from evolution models and simulations such as the kinetic Monte Carlo method. The interaction of the dislocation with defect clusters can be investigated by using atomistic molecular dynamics calculations. While in this work we adjust the CRSS to the unirradiated yield stress for each set of data, the temperature dependence of the CRSS and, as a consequence, of the yield stress, is linked to the dislocation core behavior [31] that can only be investigated by detailed first principles or molecular dynamics calculations. In this document we have provided a framework for performing physically based modeling and simulations of hardening behavior observed during irradiation. Such modeling efforts can both reproduce experimental data and also guide future experiments of irradiation hardening. Performing modeling and simulation studies before initiating an expensive neutron or proton beam experiment would prove invaluable and cost-effective.

References

[1] S.J. Zinkle, Y. Matsukawa, J. Nucl. Mater. 329–333 (2004) 88.
[2] S.A. Maloy, M.R. James, G. Willcutt, W.F. Sommer, M. Sokolov, L.L. Snead, M.L. Hamilton, F. Garner, J. Nucl. Mater. 296 (2001) 119.
[3] R.A. Lebensohn, C.N. Tome, Acta Metall. Mater. 41 (1993) 2611.
[4] U.F. Kocks, Mater. Sci. Eng. 27 (1977) 291.
[5] T.J. Koppenaal, R.J. Arsenault, Metall. Rev. (1971) 175.
[6] A. Seeger, J. Diehl, S. Mader, H. Rebstock, Philos. Mag. 2 (1957) 323.
[7] J. Friedel, Philos. Mag. 46 (1955) 1169.
[8] F. Kroupa, P.B. Hirsch, Discuss. Faraday Soc. (1964) 49.
[9] S.J. Zinkle, J. Nucl. Mater. 150 (1987) 140.
[10] P.M. Rice, S.J. Zinkle, J. Nucl. Mater. 258/263 (1998) 1414.
[11] B.N. Singh, J.H. Evans, J. Nucl. Mater. 226 (1995) 277.
[12] M.J. Makin, A.D. Whapham, F.J. Minter, Philos. Mag. 7 (1962) 285.
[13] T. Muroga, H.L. Heinisch, W.F. Sommer, P.D. Ferguson, J. Nucl. Mater. 191/194 (1992) 1150.
[14] U. Theis, H. Wollenberger, J. Nucl. Mater. 88 (1980) 121.
[15] L. Thompson, G. Youngblood, A. Sosin, Radiat. Eff. 20 (1973) 111.
[16] C.S. Deo, M.A. Okuniewski, S.G. Srivilliputhur, S.A. Maloy, M.I. Baskes, M.R. James, J.F. Stubbins, J. Nucl. Mater. 361 (2007) 141.
[17] C.S. Deo, S.G. Srinivasan, M.I. Baskes, S.A. Maloy, M. James, M. Okuniewski, J. Stubbins, J. ASTM Int. 4 (9) (2007) JAI100698.
[18] M.A. Okuniewski, D.P. Wells, F.A. Selim, S.A. Maloy, M.R. James, J.F. Stubbins, C.S. Deo, S.G. Srivilliputhur, M.I. Baskes, J. Nucl. Mater. 351 (2006) 149.
[19] Y. Dai, X.J. Jia, K. Farrell, J. Nucl. Mater. 318 (2003) 192.
[20] Y. Dai, X. Jia, J.C. Chen, W.F. Sommer, M. Victoria, G.S. Bauer, J. Nucl. Mater. 296 (2001) 174.
[21] M. Victoria, N. Baluc, C. Bailat, Y. Dai, M.I. Luppo, R. Schaublin, B.N. Singh, J. Nucl. Mater. 276 (2000) 114.
[22] C.S. Deo, M.A. Okuniewski, S.G. Srivilliputhur, S.A. Maloy, M.I. Baskes, M.R. James, J.F. Stubbins, J. Nucl. Mater. 367 (2007) 451.
[23] H. Trinkaus, B.N. Singh, J. Nucl. Mater. 323 (2003) 229.
[24] S.A. Maloy, M.R. James, G.J. Willcutt, W.F. Sommer, W.R. Johnson, M.R. Louthan Jr., M.L. Hamilton, F.A. Garner, Inst. Chem. Eng. Symp. Ser. (2000) 644.
[25] Y. Dai, X. Jia, M. Victoria, J. Nucl. Mater. 305 (2002) 1.
[26] G.R. Odette, J. Nucl. Mater. 215 (1994) 45.
[27] G.R. Odette, T. Yamamoto, H.J. Rathbun, M.Y. He, M.L. Hribernik, J.W. Rensman, J. Nucl. Mater. 323 (2003) 313.
[28] A. Arsenlis, B.D. Wirth, M. Rhee, Philos. Mag. 84 (2004) 3617.
[29] B.N. Singh, A.J.E. Foreman, H. Trinkaus, J. Nucl. Mater. 249 (1997) 103.
[30] B.N. Singh, N.M. Ghoniem, H. Trinkaus, J. Nucl. Mater. 307 (2002) 159.
[31] M. Duesbery, V. Vitek, Acta Mater. 46 (1998) 1481.